RSC Advances

PAPER

View Article Online
View Journal | View Issue

Cite this: *RSC Adv.*, 2026, **16**, 6612

Synthesis of some new pyrene-based hydrazinyl-thiazole derivatives *via* a one-pot strategy: biological evaluation and molecular docking studies

Pramod Dinkar Jawalepatil,†*[a] Amol Maruti Jadhav, †*[b] Pritam Bhagwan Bhosale,[c] Pooja Singh,[d] Hyun Ho Choi,*[be] Sang Yong Nam, *[be] Mahesh Narayan Waman,[f] Gajanan Namdeo Wadje[f] and Satish Uttamrao Deshmukh *[f]

In this study, we report a streamlined one-pot synthesis of a new series of (*E*)-4-phenyl-2-(2-(pyren-1-ylmethylene)hydrazinyl)thiazole derivatives (**4a–4o**). The reaction involves the condensation of pyrene-1-carbaldehyde, thiosemicarbazide, and α-halo ketones in the presence of a catalytic amount of $InCl_3$ as a Lewis acid catalyst, carried out under reflux in a (1 : 1, v/v) H_2O/EtOH medium at 80 °C. This protocol provides several key advantages, including mild reaction conditions, short reaction times, excellent yields, broad functional group tolerance, and the added benefit of chromatography-free product isolation, thereby enhancing practicality and operational simplicity. All synthesized compounds were fully characterized using ^{1}H NMR, ^{13}C NMR, FT-IR spectroscopy, and LC-MS analysis. The anticancer potential of the synthesized derivatives was evaluated against the human breast cancer cell line (MCF-7) using an *in vitro* MTT assay. Compounds **4m** and **4g** exhibited the most promising cytotoxic effects, displaying IC_{50} values of 43.66 and 45.24 μg mL^{-1}, respectively. Furthermore, molecular docking studies were performed to elucidate structure–activity relationships, revealing a strong correlation between the predicted binding affinities and the experimental biological outcomes.

Received 22nd December 2025
Accepted 19th January 2026

DOI: 10.1039/d5ra09880g

rsc.li/rsc-advances

1 Introduction

The development of more effective and ecologically friendly synthetic processes has received a lot of attention recently.[1,2] Multicomponent reactions (MCRs) have emerged as powerful tools for an efficient synthesis of complex molecules. These reactions involve the simultaneous condensation of three or more reactants in a single step, minimizing waste and improving atom economy.[3–6] MCRs are particularly advantageous in medicinal chemistry, where the demand for efficient, sustainable, and high-throughput compound libraries continues to rise. MCR is key class of heterocyclic compounds that are frequently explored through the bioactive scaffold of thiazoles.[7,8] These five-membered aromatic rings, containing both nitrogen and sulfur atoms, are well-known for their pharmacological versatility.[9–11] The sulfur atom, in particular, can engage in critical interactions with biological receptors, enhancing binding affinity and therapeutic efficacy.[12] The thiazole moiety is a common structural motif in numerous natural and synthetic bioactive compounds, including thiamine (vitamin B1),[13] penicillin,[14] and micrococcins.[15] Additionally, thiazole derivatives feature in clinically approved drugs such as fanetizole,[16] ritonavir,[17,18] dasatinib,[19] ravuconazole,[20,21] nizatidine,[22] meloxicam,[23] and niridazole[24] underscoring their relevance in drug design as shown in (Fig. 1). Recent studies continue to highlight the importance of pyrene and pyrene-based heterocycles in medicinal chemistry. Mohammed *et al.* reported a series of pyrimidine-pyrene/benzochromene hybrid derivatives that exhibited potent anticancer activity against HCT-116 cells, supported by molecular docking studies revealing key interactions within the EGFR binding site. Similarly, Paul *et al.* synthesized pyrene-appended Schiff base tin(IV) complexes that demonstrated significant cytotoxic effects and

[a]*Department of Chemistry, Balbhim Arts, Science and Commerce College, Beed 431122, MS, India. E-mail: pramodjawalepatil@gmail.com*

[b]*Research Institute of Green Energy, and Convergence Technology (RIGET), Gyeongsang National University, Jinju 52828, South Korea. E-mail: amolj848@gmail.com*

[c]*Department of Veterinary Medicine, Research Institute of Life Science, Gyeongsang National University, 501 Jinju-daero, Jinju, 52828, Republic of Korea*

[d]*Division of Applied Life Science, (BK21 Four), Plant Molecular Biology and Biotechnology Research Center (PMBBRC), Gyeongsang National University (GNU), 501 Jinju-Daero, Jinju, 52828, Republic of Korea*

[e]*Department of Materials Engineering and Convergence Technology, Gyeongsang National University, Jinju 52828, Republic of Korea. E-mail: hh.choi@gnu.ac.kr; walden@gnu.ac.kr*

[f]*Department of Chemistry, Deogiri College, Aurangabad, Maharashtra 431005, India. E-mail: satishud@gmail.com*

† These authors contributed equally to this work.

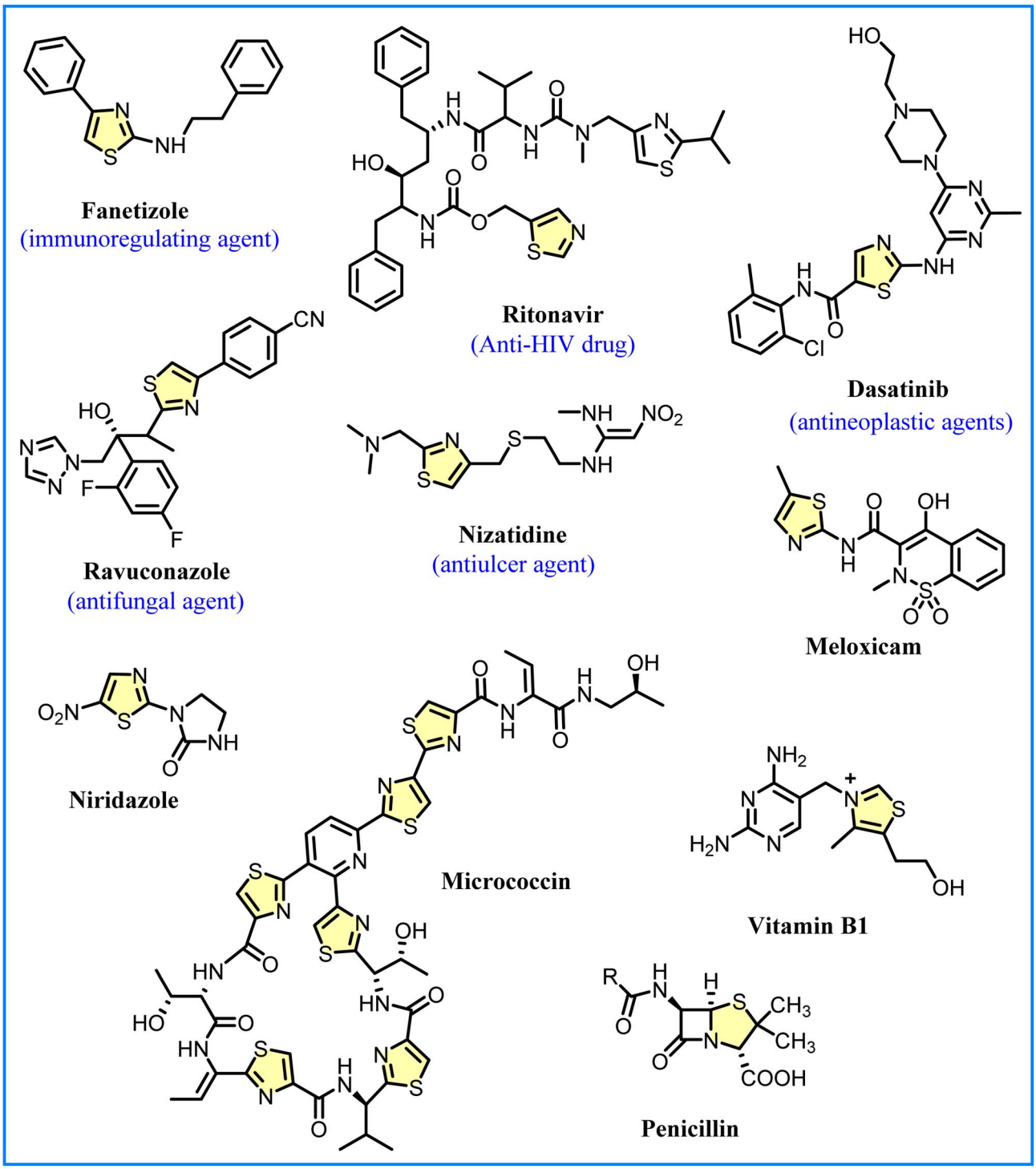

Fig. 1 Examples of natural and synthetic bioactive molecules with thiazole and hydrazinyl linkages.

provided valuable docking insights into protein–ligand interactions.[25] In this context, the Pyrene-based Hydrazinyl-Thiazole (PHT) scaffold has become a favourite pharmacophore, attracting significant attention from industrial and pharmaceutical researchers because of its diverse biological potential. Beyond their therapeutic applications, thiazoles have also been explored in the field of material science, particularly in the development of organic semiconductors and fluorescence-based sensors.[26] This multifunctionality is further enhanced by fluorination, a strategic modification that significantly impacts the pharmacokinetic and physicochemical properties of molecules.[27] The incorporation of fluorine atoms especially trifluoromethyl groups can improve membrane permeability, metabolic stability, bioavailability, and target specificity.[28–30] As a result, more than 20% of FDA-approved drugs now contain at least one fluorine atom.[31] Notably, trifluoromethylated

Previous works:

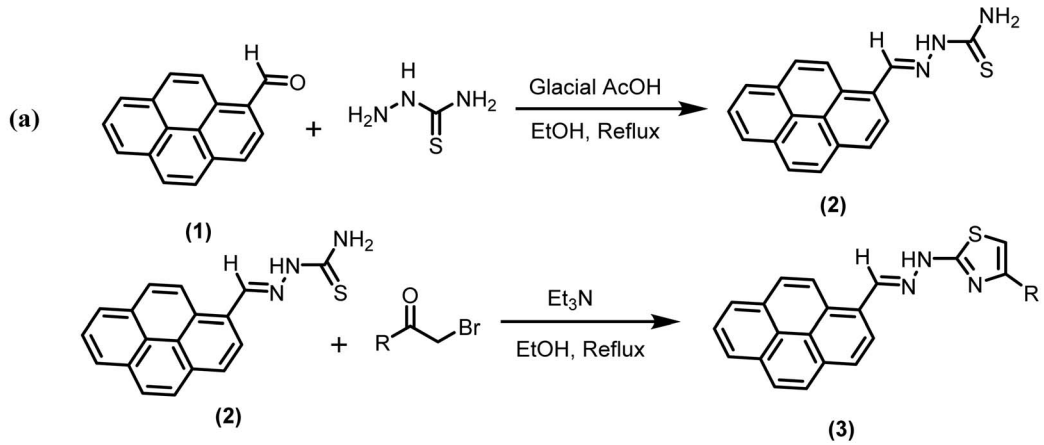

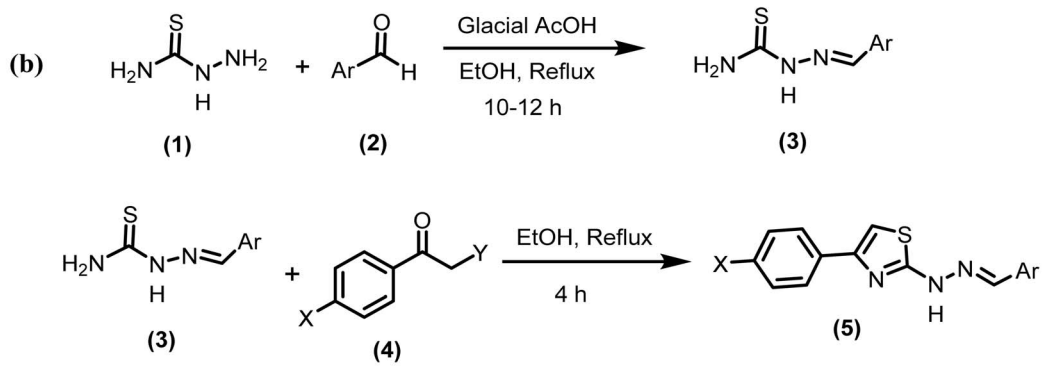

Present work:

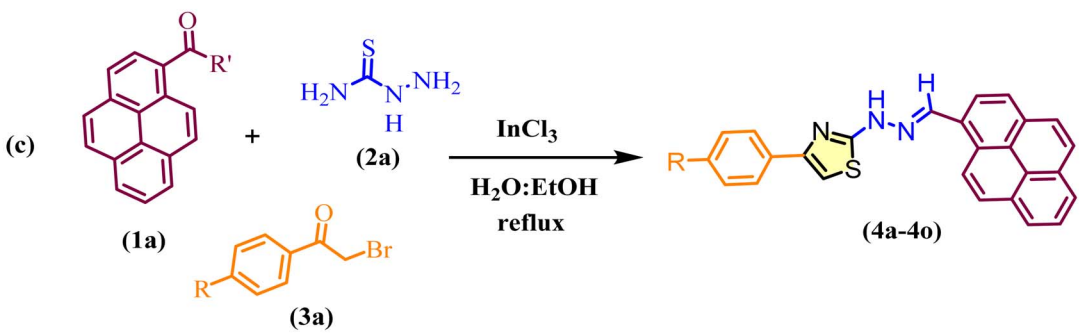

Scheme 1 $InCl_3$-catalyzed routes to the pyrene-hydrazinyl-thiazole (PHT) scaffold: (a, b) literature methods and (c) the present one-pot synthesis of compounds (4a–4o).

compounds such as flutamide, hydroxyflutamide, nilutamide, and 5-trifluoromethyl uracil are extensively used in the treatment of metastatic prostate cancer,[32] reflecting the growing relevance of fluorinated molecules in oncology. Another promising structural unit is pyrene; a symmetrical tetracyclic aromatic hydrocarbon composed of 16 π-electrons.[33,34] Typically

derived from the combustion of organic material, pyrene is widely studied for its luminescent and photophysical properties.[35] Its unique vibronic emission patterns and prolonged fluorescence lifetime make it a valuable probe in biological imaging, chemical sensing, and materials science.[36–38] Moreover, pyrene derivatives bearing sugar moieties or heterocyclic extensions have demonstrated antiviral activity, particularly against HSV-1 and HIV-1, expanding their therapeutic significance.[39,40]

Cancer remains one of the most serious global health challenges, characterized by complex interactions between environmental, genetic, and biochemical factors.[41] Despite substantial advancements in cancer research, many existing therapies lack selectivity and often cause significant toxicity to healthy tissues.[42,43] In this context, the development of targeted anticancer agents with minimal off-target effects is an urgent priority. Among the most commonly used models for evaluating anticancer efficacy is the MCF-7 breast cancer cell line, which is representative of hormone-responsive human breast adenocarcinoma.[44] To address this, we designed and synthesized some new series of (PHT) derivatives *via* a one-pot multicomponent synthetic approach. These compounds were structurally optimized to incorporate pharmacologically significant fragments, including trifluoromethyl groups and pyrene moieties, with the aim of enhancing their cytotoxic potential against MCF-7 cells. Furthermore, to investigate the mechanism of action and binding potential, we employed molecular docking simulations targeting monoamine oxidase A (MAO-A), an enzyme implicated in both neurological disorders and cancer progression.[45,46] Clorgyline, a well-characterized selective MAO-A inhibitor, was used as a reference to benchmark binding affinities.[47,48] Docking studies offer critical insights into ligand receptor interactions, enabling the prediction of binding orientation, interaction energies, and key contact residues within the enzyme's active site. This computational approach is a cornerstone of rational drug design and plays a pivotal role in accelerating the discovery of bioactive compounds.[49–52]

Therefore, the development of a rapid and efficient synthetic route to access physiologically active (PHT) molecules remains highly desirable. In our previous related works (Scheme 1a and b), Channar *et al.* and Salar *et al.*[53] reported synthetic strategies that required multi-step reaction sequences, provided moderate-to-low yields, and relied on toxic organic solvents and catalysts. Das *et al.* reported thiazole derivatives supported by molecular docking studies; however, their synthetic protocol required column chromatography, employed toxic catalysts and solvents, and involved a relatively complex workup procedure.[54] These limitations motivated us to develop a simplified and operationally convenient one-pot strategy for constructing pyrene-based hydrazinyl-thiazole (PHT) derivatives. Although several methodologies have been reported for the synthesis of thiazole frameworks including ionic liquid-mediated processes, graphene oxide catalysis, visible-light activation, and Brønsted acid catalysis none of these approaches address the specific construction of pyrene-based hydrazinyl-thiazole scaffolds.[54] Notably, literature lacks a one-pot multicomponent protocol combining pyrene-1-carbaldehyde, thiosemicarbazide, and aryl phenacyl bromides, and no reports describe an indium(III) chloride-promoted hydrazinyl-thiazole formation in an aqueous-ethanol medium. Moreover, previously published strategies generally rely on chromatographic purification, whereas the present method offers chromatography-free product isolation, further enhancing its practicality. These considerations underscore the novelty, efficiency, and operational advantages of the synthetic protocol presented in this study.

As part of our ongoing efforts to develop efficient and practical synthetic methodologies,[55] we now report a one-pot, multicomponent condensation strategy for the synthesis of several new (PHT) derivatives. This protocol utilizes pyrene-1-carbaldehyde, thiosemicarbazide, and *p*-chlorophenacyl bromide in the presence of a catalytic amount of indium(III) chloride ($InCl_3$), performed in a (1 : 1, v/v) water–ethanol solvent system at 80 °C (Scheme 1c). The synthesized compounds were subsequently evaluated for their anticancer potential through *in vitro* biological assays and molecular docking studies. Particular attention was given to their selective cytotoxicity against the MCF-7 breast cancer cell line and their inhibitory activity toward monoamine oxidase A (MAO-A).[55]

2 Results and discussion

2.1 Chemistry

We first tried to synthesise of (*E*)-4-(4-chlorophenyl)-2-(2-(pyren-1-ylmethylene)hydrazinyl)thiazole (**4a**) from pyrene-1-carbaldehyde (**1a**), thiosemicarbazide (**2a**), and *p*-chlorophenacyl bromide (**3a**) as a model study in (Scheme 2). A variety of catalysts, solvents, temperatures, and reaction periods were methodically investigated to optimise the reaction conditions. The results of the optimizations are summarized in (Table 1). Initially, the reaction was conducted in ethanol at 80 °C without a catalyst, and even after 20 hours, only trace amounts of the desired product were produced (Table 1, entry 1). The addition of various acid, Brønsted and Lewis acid catalysts such as *p*-TSA, and L-proline improved the yields slightly, with L-proline offering up to 40% yield (Table 1, entries 2 and 3). Similarly, a representative reaction was carried out with transition metal salts such as ZnO, $Cu(OTf)_2$, $NiCl_2$, and $GaCl_3$ afforded moderate yields ranging between 25–35% (Table 1, entries 4–7). Among them, $Sc(OTf)_3$ gave the best result in ethanol with a yield of 45% (Table 1, entry 9). With these unsatisfactory results, we moved on Lewis acid indium(III) chloride ($InCl_3$) at 10 mol% in ethanol at 80 °C led to a better yield of 60% in just 6 hours (Table 1, entry 9). Encouraged by this result, we evaluated the effect of solvent systems using $InCl_3$ as a catalyst. The reaction was then conducted in different solvents under reflux conditions. Notably, using a (1 : 1, v/v) mixture of water and ethanol (H_2O : EtOH) as the solvent dramatically enhanced the reaction efficiency, affording compound **4a** in 98% yield within just 2 hours (Table 1, entry 10). This result highlights the offering a noticeable of solvent polarity and the solubility of reactants in driving the transformation efficiently. In contrast, other solvents, including protic solvents such as methanol (MeOH) trifluoroethanol (TFE), isopropanol (i-PrOH) and water

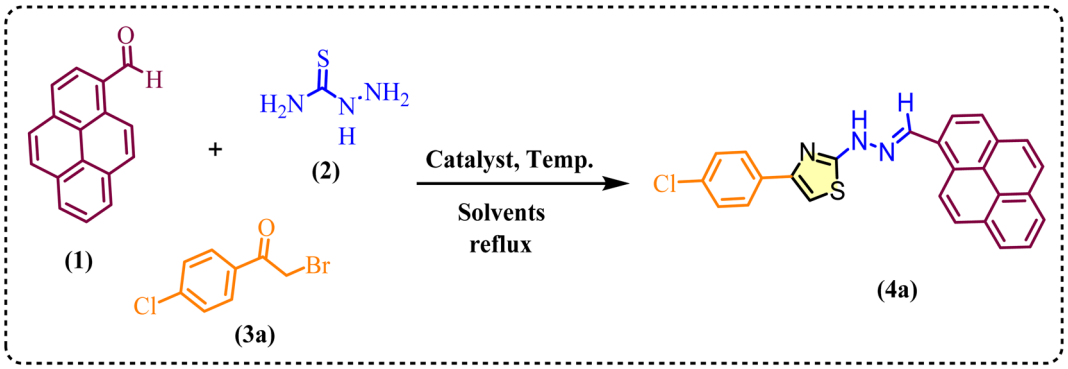

Scheme 2 $InCl_3$ Catalyzed synthesis of pyrene-hydrazinyl-thiazole (PHT) Scaffold.

Table 1 Optimization of reaction conditions for the synthesis of pyrene-hydrazinyl-thiazole (**4a**)[a]

Sr. no.	Catalyst (mol%)	Solvents	Temp. (°C)	Time (h)	Yield[b] (%)
1	—	EtOH	80	20	Trace
2	*p*-TSA (10%)	EtOH	80	14	30
3	L-Proline (10%)	EtOH	80	12	40
4	ZnO (10%)	EtOH	80	16	—
5	$Cu(OTf)_2$ (10%)	EtOH	80	10	30
6	$NiCl_2$ (10%)	EtOH	80	10	25
7	$GaCl_3$ (10%)	EtOH	80	8	35
8	$Sc(OTf)_3$ (10%)	EtOH	80	10	45
9	$InCl_3$ (10%)	EtOH	80	6	60
10	$InCl_3$ (10%)	H_2O : EtOH	Reflux	2	98
11	$InCl_3$ (10%)	MeOH	Reflux	6	48
12	$InCl_3$ (10%)	H_2O	Reflux	10	Traces
13	$InCl_3$ (10%)	Toluene	Reflux	10	36
14	$InCl_3$ (10%)	CH_3CN	Reflux	8	40
15	$InCl_3$ (10%)	DCM	Reflux	12	Traces
16	$InCl_3$ (20%)	H_2O : EtOH	Reflux	2	96
17	$InCl_3$ (30%)	H_2O : EtOH	Reflux	2.5	92
18	$InCl_3$ (5%)	H_2O : EtOH	Reflux	3	78
19	$InCl_3$ (10%)	i-PrOH	Reflux	9	35
20	$InCl_3$ (10%)	TFE	Reflux	8	48

[a] Reaction conditions: pyrene-1-carbaldehyde (**1a**, 1 mmol), thiosemicarbazide (**2a**, 1 mmol) and *p*-chlorophenacyl bromide (**3a**, 1 mmol) were reacted in the presence of $InCl_3$ (10 mol%) under reflux in H_2O : EtOH (1 : 1, v/v). [b] Isolated yields of purified products.

(H_2O), and aprotic solvents such as toluene, acetonitrile (CH_3CN), and dichloromethane (DCM), were less effective, affording yields of 20–48% or only trace amounts in some cases (Table 1, entries 11–15, 19 and 20). These observations suggest that the H_2O : EtOH (1 : 1) solvent mixture is optimal for the dissolution and reactivity of all three components. We further explored the effect of increasing the catalyst loading of $InCl_3$. Moreover, the reaction yield was strongly influenced by the amount of $InCl_3$ employed. When catalyst loadings of 5, 10, 20, and 30 mol% were used, the corresponding yields were 78%, 98%, 96%, and 92%, respectively (Table 1, entries 10 and 16–18). Therefore, 10 mol% of $InCl_3$ in H_2O : EtOH under reflux was deemed the optimal condition. These results demonstrate that the choice of catalyst and solvent is critical to achieving high yields in the one-pot cascade reaction.

When various substrates were exposed to the ideal reaction conditions, the intended products were produced in high yields (Table 2). In a one-pot process, pyrene-1-carbaldehyde, different *p*-chlorophenacyl bromides, and thiosemicarbazide were used to create a series of pyrene-hydrazinyl-thiazole derivatives (**4a–4o**), with indium(III) chloride ($InCl_3$) acting as an effective and reusable catalyst. The reactions took place in a water–ethanol combination (1 : 1 v/v) under benign, eco-friendly conditions. The reaction conditions allowed for the high tolerance of a broad variety of functional groups on the aromatic ring of *p*-chlorophenacyl bromide. In addition, electron-donating groups like methyl and methoxy (Table 2, entries **4b** and **4g**) and electron-withdrawing substituents like bromo, chloro, fluoro, nitro, trifluoromethyl, and trifluoromethoxy (Table 3, entries **4f**, **4a**, **4e**, **4n**, **4o**, **4c**, **4d**, **4i**, **4m**, and **4k**) were well tolerated without sacrificing reaction efficiency. Furthermore, the substrate scope was extended to include sterically and electronically diverse aryl systems, as exemplified by thiophenyl, biphenyl, and naphthyl (Table 2, entries, **4h**, **4i** and **4j**) derivatives, highlighting the

Table 2 Substrate scope of pyrene-hydrazinyl-thiazole Scaffolds using $InCl_3$ (**4a–4o**)[a,b]

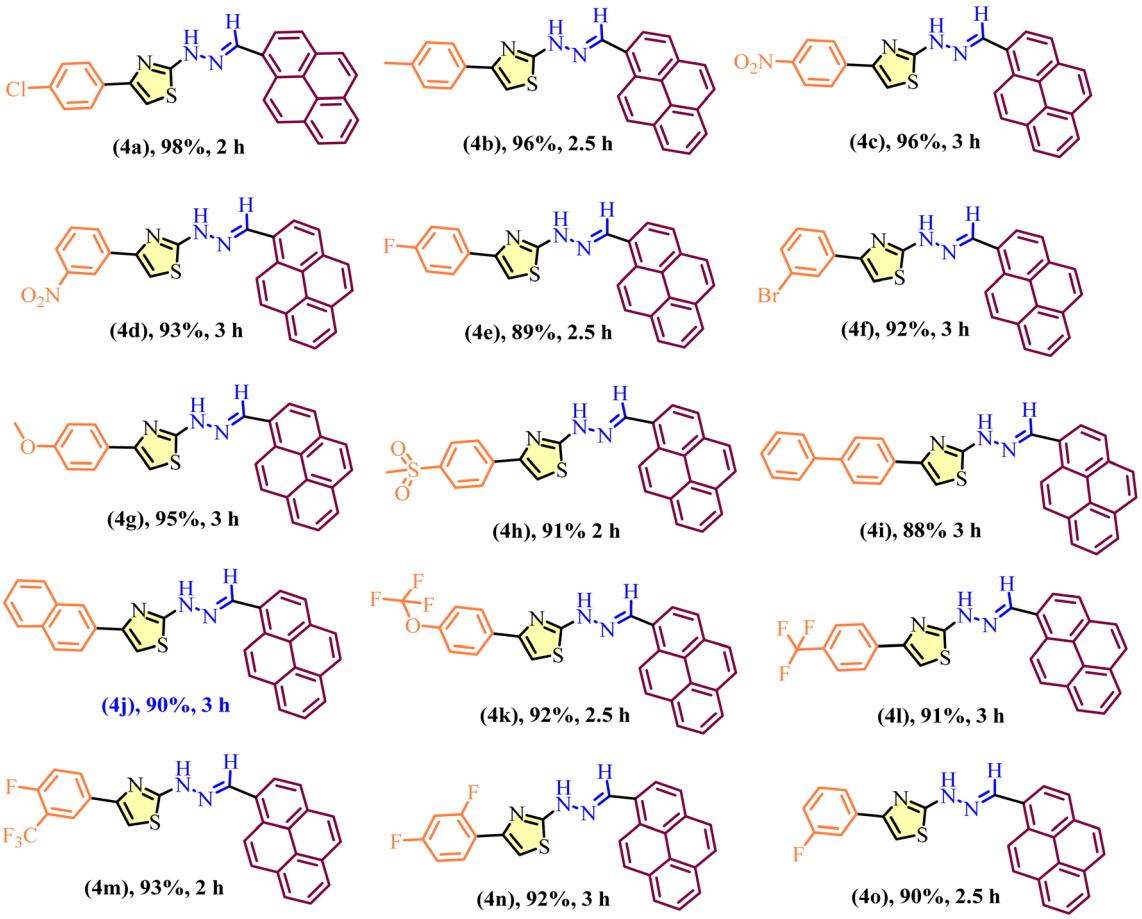

[a] Reactions were carried out for pyrene-hydrazinyl-thiazole Scaffolds, pyrene-1-carbaldehyde (1 mmol), thiosemicarbazide (1 mmol), and various *p*-chlorophenacyl bromide (1 mmol) in the presence of water : ethanol (1 : 1 v/v) and 10 mg of $InCl_3$ catalyst. [b] Isolated yields.

robustness and generality of the developed protocol. Overall, the reactions proceeded cleanly without the formation of any detectable side products. These compounds were then tested in the lab for their ability to fight cancer, and they were also analyzed using molecular docking studies against Monoamine Oxidase A (MAO-A) to explore their biological potential. The structures of all synthesized compounds (**4a–4o**) were confirmed using spectroscopic and analytical techniques,

Table 3 Molecular docking analysis

Sr. no.	Samples name	CDOCKER interaction energy	H-bond forming residues
1	Clorgyline (REF)	−17.45	Thr336
2	**4a**	−28.72	None
3	**4b**	−84.81	Met445
4	**4c**	−41.69	Ile23
5	**4d**	−51.30	Ile23, Thr52
6	**4e**	−31.78	Met445
7	**4f**	−82.09	Tyr444
8	**4g**	−45.87	Gln215, Tyr444
9	**4h**	−57.47	Val210, Gln215, Cys323, Tyr444
10	**4j**	−64.75	Gln215, Tyr444
11	**4k**	−66.85	Arg51, Thr52
12	**4l**	−47.84	Val210, Gln215, Cys323, Tyr444
13	**4m**	−67.01	Gln215, Cys323, Tyr444
14	**4n**	−31.80	Ile23, Met445
15	**4o**	−41.77	Val210

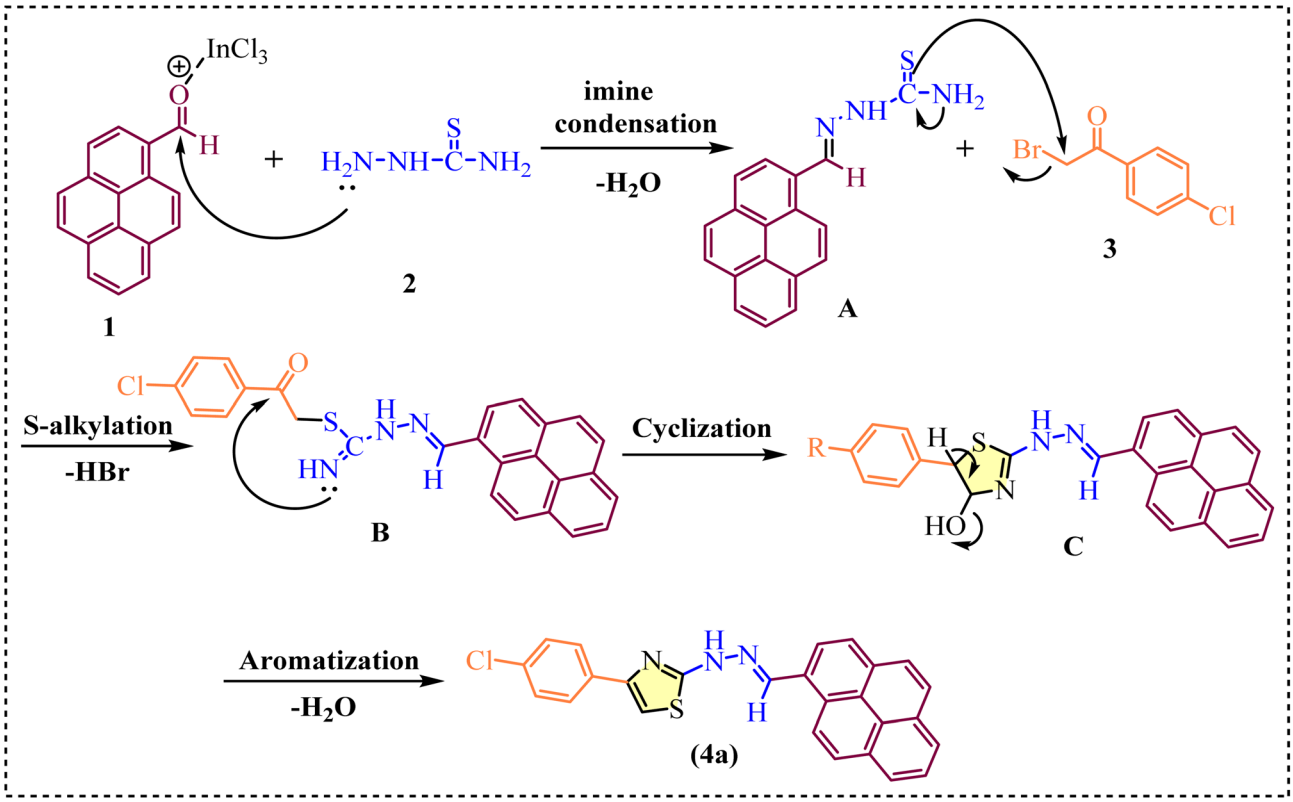

Fig. 2 Proposed reaction mechanism for the $InCl_3$-catalyzed one-pot synthesis of pyrene-hydrazinyl-thiazole derivative (**4a**).

including ^1H, ^{13}C NMR, ^{19}F NMR, FT-IR, and LC-MS analysis as provided in the SI (Fig. S9–S74).

A plausible mechanism for the $InCl_3$-catalyzed one-pot synthesis of pyrene-hydrazinyl-thiazole derivatives is outlined in (Fig. 2). Initially, activation of pyrene-1-carbaldehyde (**1**) occurs through coordination of the carbonyl oxygen with the Lewis acidic $InCl_3$ catalyst, which increases the electrophilicity of the aldehyde carbon. This activated aldehyde then undergoes imine condensation with thiosemicarbazide (**2**), accompanied by the elimination of a water molecule, to afford the corresponding hydrazone intermediate **A**. Subsequently, intermediate **A** reacts with the α-haloketone (**3**) *via S*-alkylation, wherein the nucleophilic sulfur atom attacks the electrophilic carbon bearing the halogen, leading to the formation of intermediate **B** with the release of HBr. The enhanced electrophilicity of the α-haloketone is further facilitated by $InCl_3$ coordination, promoting efficient alkylation. Intermediate **B** then undergoes an intramolecular cyclization through nucleophilic attack of the hydrazinyl nitrogen onto the carbonyl carbon, forming the thiazoline-type intermediate **C**. Finally, aromatization of intermediate **C** occurs *via* dehydration, yielding the thermodynamically stable pyrene-hydrazinyl-thiazole derivative **4a**.

3 *In silico* study

3.1 Target prediction

The target prediction analysis of the query molecules, based on structural similarity to known bioactive compounds, revealed potential interactions with a diverse range of protein targets across multiple target classes. As illustrated in the pie chart, the top 15 predicted targets span various protein families, including oxidoreductases (20.0%), enzymes (20.0%), kinases (20.0%), G protein-coupled receptors (13.3%), transcription factors (6.7%), proteases (6.7%), and other nuclear proteins (6.7%). Among these, monoamine oxidase A (MAO-A) and monoamine oxidase B (MAO-B) were identified as the most likely targets for the majority of compounds, supported by a high number of known active compounds showing strong 3D and 2D similarity to the query structures as shown in SI (Fig. S3).

3.2 Molecular docking

The co-crystal structure of the MAO-A protein with clorgyline (PDB ID: 1O5W) was used as the target receptor to perform molecular docking (MD) studies. The structure was prepared in Discovery Studio (DS v2023) by removing heteroatoms, and the binding site was defined using the define and edit binding site module within the cavity of the co-crystallized inhibitor clorgyline (REF). The *XYZ* coordinates were set as 39.19, 27.41, and −16.14, with the docking sphere radius defined within 12 Å. Molecular docking of the synthesized thiazole derivatives (**4a–4o**) was carried out using the CDOCKER module of DS. Docking validation was confirmed by redocking the REF into the same binding cavity before performing the actual MD studies. The selective MAO-A inhibitor clorgyline (REF) displayed a CDOCKER interaction energy of −17.45. Therefore, compounds exhibiting more negative CDOCKER interaction energies than REF were considered potential MAO-A inhibitors. As shown in (Table 3), all

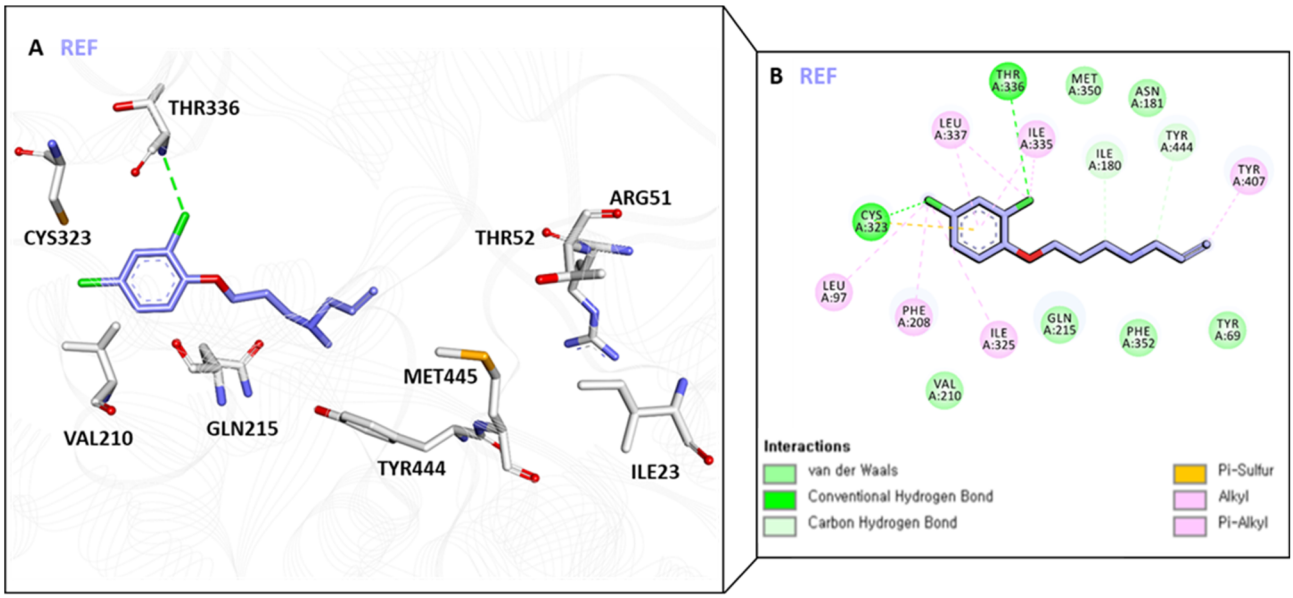

Fig. 3 Molecular docking of the reference compound (REF) in the MAO-A active site: (A) 3D binding pose and (B) 2D interaction map showing key hydrogen bonding and hydrophobic interactions.

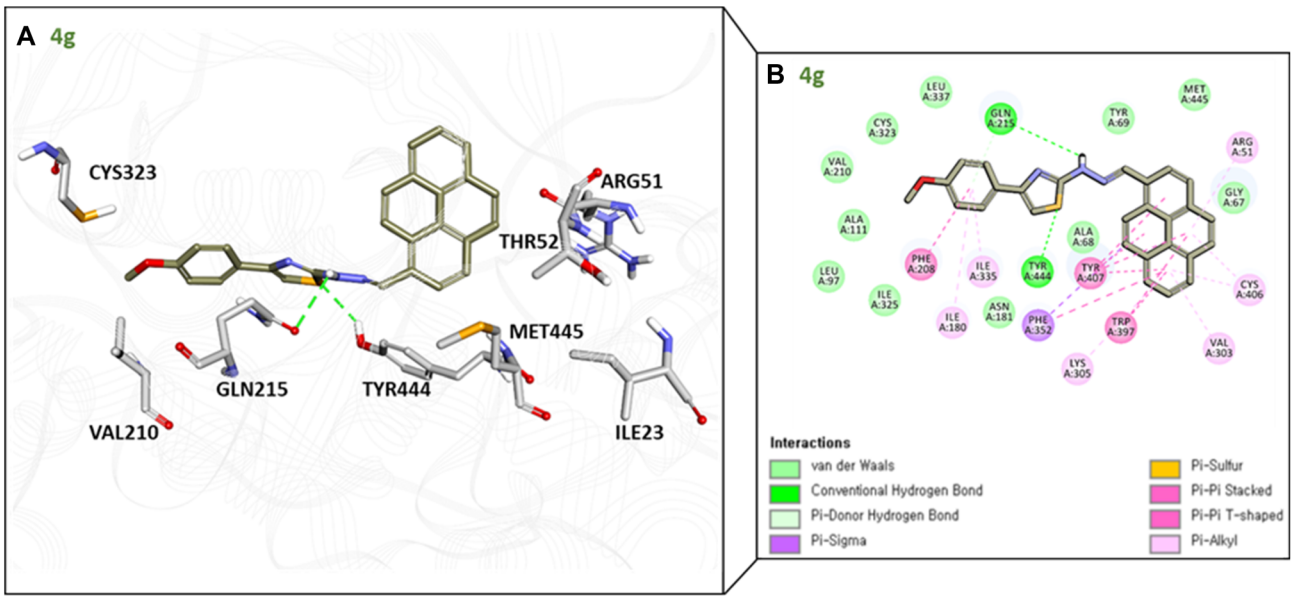

Fig. 4 Molecular docking interactions of compound **4g** within the MAO-A active site: (A) 3D binding pose and (B) 2D interaction map showing key hydrogen bonding and hydrophobic interactions.

synthesized compounds displayed stronger binding affinities compared with the REF, with **4b** (−84.81), **4f** (−82.09), **4m** (−67.01), and **4k** (−66.85) showing the highest binding scores. Hydrogen bonding interactions were observed with polar residues such as Arg51, Thr52, Gln215, Cys323, and Tyr444, while hydrophobic and van der Waals interactions were established with Ile23, Val210, and Met445, collectively contributing to stabilization of the ligand–receptor complex. Notably, compounds **4g**, **4h**, and **4m** formed multiple hydrogen bonds within the MAO-A active site, further enhancing their binding potential. Based on detailed molecular interaction analysis, **4g** and **4m** were shortlisted as the most promising lead compounds for further evaluation. The CDOCKER scores and hydrogen bond-forming residues of all docked molecules are summarized in (Table 3), while the detailed 2D and 3D interaction diagrams of the final selected hits are presented in (Fig. 3–5). Additional 2D molecular docking interaction maps for the synthesized compounds (**4a–4o**) and the reference compound, as well as the 3D interaction maps of the selected compounds (**4h**, **4j**, **4k**, **4l**, and **4n**), are provided in the SI (Fig. S5, S7 and S8).

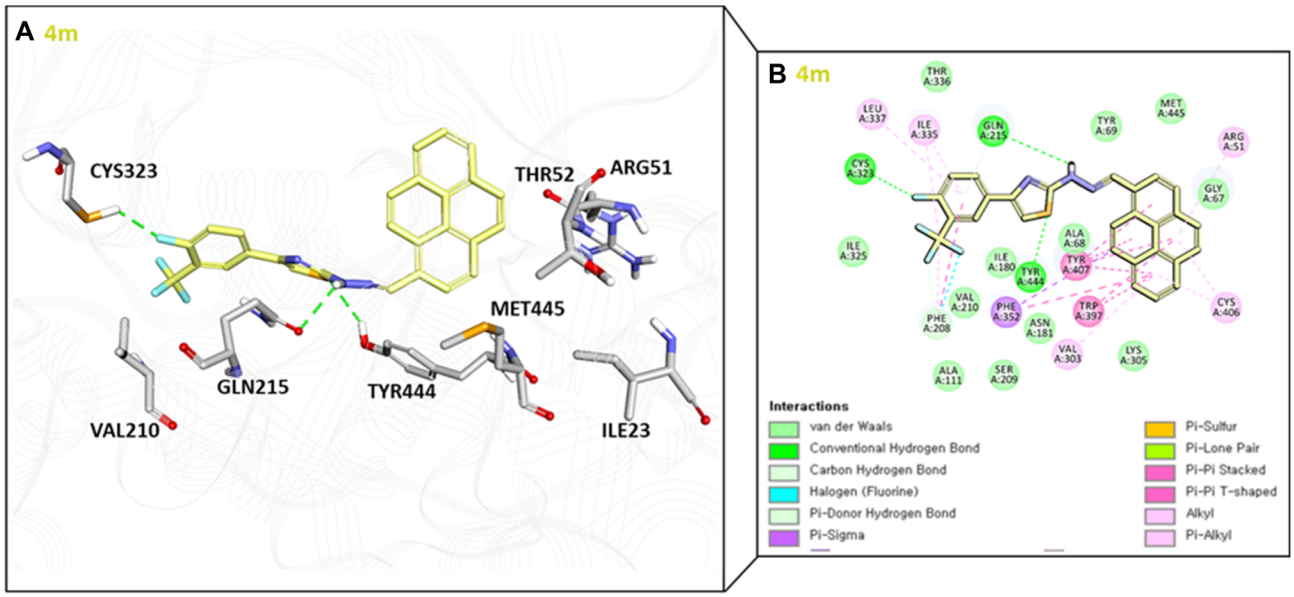

Fig. 5 Molecular docking interactions of compound **4m** in the MAO-A active site: (A) 3D binding pose and (B) 2D interaction map highlighting key hydrogen bonding and hydrophobic interactions.

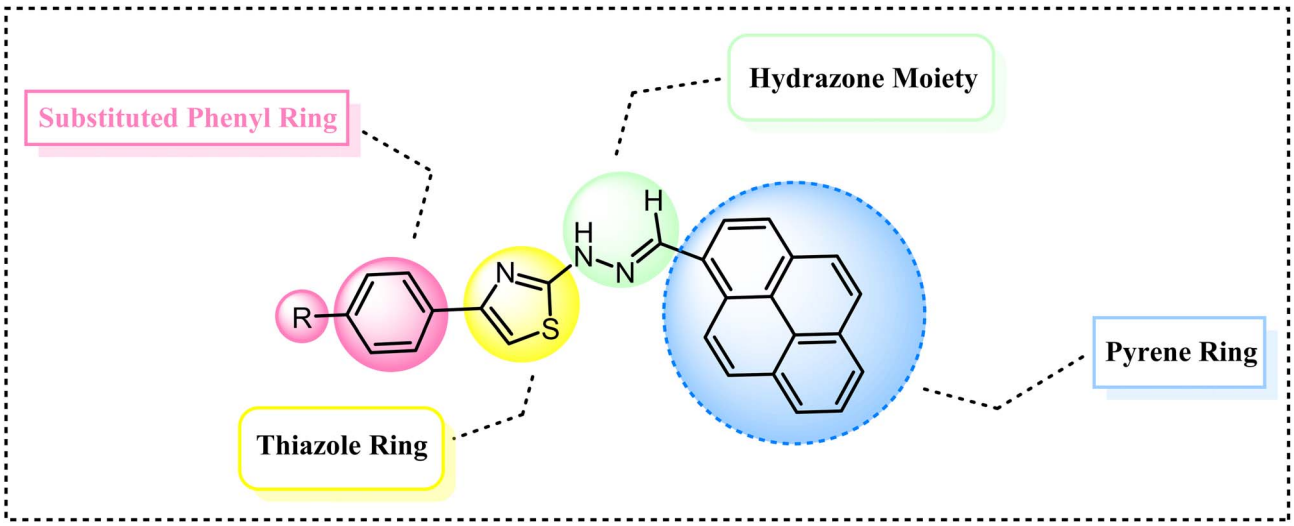

Fig. 6 The structure–activity relationship (SAR) of one-pot synthesized pyrene-hydrazinyl-thiazole derivatives.

3.3 Structure–activity relationship (SAR)

The structure–activity relationship (SAR) analysis of the synthesized pyrene-hydrazinyl-thiazole derivatives demonstrates that their anticancer activity is highly dependent on specific structural features within the molecular framework. As illustrated in (Fig. 6), all compounds share a common pharmacophoric scaffold composed of four key regions: (i) a substituted aryl ring, (ii) a thiazole linker, (iii) a hydrazone moiety, and (iv) a polycyclic aromatic pyrene unit. Structural variations within these regions significantly influence the observed cytotoxic behavior. Notably, compounds **4m** and **4g** exhibited the most promising anticancer activity against the MCF-7 cell line, with IC_{50} values of 43.66 and 45.24 μg mL^{-1}, respectively. A clear trend was observed with respect to the electronic nature of substituents on the aryl ring (highlighted in pink). Derivatives bearing electron-withdrawing groups (EWGs) such as $-CF_3$, –F, –Cl, and –Br generally showed enhanced cytotoxic activity compared to those containing electron-donating groups (EDGs). In particular, the superior activity of compound **4m**, containing a trifluoromethyl substituent, can be attributed to the strong electron-withdrawing effect and increased lipophilicity, which favor improved hydrophobic interactions and optimal accommodation within the target protein's binding pocket. In contrast, compounds bearing electron-donating substituents displayed comparatively moderate activity, likely due to reduced binding affinity and less effective hydrophobic interactions. The thiazole linker (yellow region) plays

Table 4 Cytotoxic activity of the synthesized compounds against the MCF-7 cells

Comp.	1.56 μg mL^{-1}	3.125 μg mL^{-1}	6.25 μg mL^{-1}	12.5 μg mL^{-1}	25 μg mL^{-1}	50 μg mL^{-1}	100 μg mL^{-1}	IC_{50} μg mL^{-1}
4g	4.493	8.837	15.68	33.06	54.75	60.23	69.66	45.24
4h	8.739	11.93	41.56	42.33	49.95	46.68	23.68	50.04
4j	0.8966	29.79	37.10	44.95	32.96	27.10	14.28	55.04
4k	10.36	17.70	18.85	20.84	25.04	30.33	48.56	51.43
4l	28.71	31.51	31.14	39.46	46.19	49.76	49.58	50.23
4m	39.35	41.78	46.39	56.33	46.74	45.09	37.08	43.66
4n	9.508	19.22	29.73	46.78	58.17	60.28	72.39	53.22

a crucial role in maintaining molecular rigidity and π-conjugation, enabling effective π–π stacking interactions with aromatic amino acid residues in the enzyme binding pocket, such as MAO-A. This rigidified scaffold helps preserve an optimal binding geometry, thereby contributing to improved biological efficacy. The hydrazone moiety (green region), containing both hydrogen bond donor (–NH) and acceptor (=N–) functionalities, is essential for establishing stabilizing hydrogen-bonding interactions with key residues of the biological target, as supported by molecular docking studies. Finally, the pyrene unit (blue region) significantly contributes to the overall hydrophobic character and biological performance of the compounds. Its extended planar π-system facilitates π-surface interactions and van der Waals contacts within the protein binding cavity, while also potentially enhancing membrane permeability and cellular uptake. Collectively, the SAR findings reveal that the superior cytotoxic activity observed for compounds **4g** and **4m** arises from the synergistic interplay of electron-withdrawing aryl substitution, rigid thiazole linkage, hydrogen-bond-capable hydrazone moiety, and the hydrophobic pyrene core. These insights provide a rational basis for further structural optimization aimed at improving potency and selectivity of pyrene-hydrazinyl-thiazole-based anticancer agents.

3.4 Cytotoxic activity

3.4.1. Anticancer screening of the synthesized compounds. The MTT assay is a colorimetric technique widely used to evaluate cell viability and metabolic activity.[57] The MCF-7 human breast cancer cell line (Michigan Cancer Foundation-7) was originally derived in 1973 from the pleural effusion of a patient with metastatic invasive ductal carcinoma and has since been established as a commonly used *in vitro* model for estrogen receptor-positive (ER^+) breast cancer.[58] The MCF-7 human breast cancer cell line was selected for this study due to its well-characterized molecular profile, widespread use in anticancer drug screening, and its relevance in evaluating compounds targeting hormone-dependent breast cancer. MCF-7 cells are classified as a luminal A subtype, as they express estrogen and progesterone receptors (ER and PR), lack HER2 overexpression, and retain wild-type TP53.[59] Morphologically, these cells exhibit epithelial-like characteristics and proliferate as adherent monolayers with a relatively slow doubling time. Owing to their hormone responsiveness, low metastatic potential, and clinical relevance, MCF-7 cells are considered a gold-standard model for ER-positive breast cancer and are widely employed in studies related to estrogen signaling, endocrine therapy, drug resistance, and the cytotoxic screening of novel anticancer agents.[60] In addition, the lack of functional caspase-3 in MCF-7 cells results in altered apoptotic responses, facilitating the distinction of cytostatic effects, cell-cycle arrest, and alternative cell death pathways. Furthermore, the concentrations of the synthesized compounds required to inhibit 50% of the malignant cell population (IC_{50}) were determined.[56] MCF-7 cells were treated with a concentration gradient of each compound (100, 50, 25, 12.5, 6.25, 3.125, and 1.56 μg mL^{-1}),

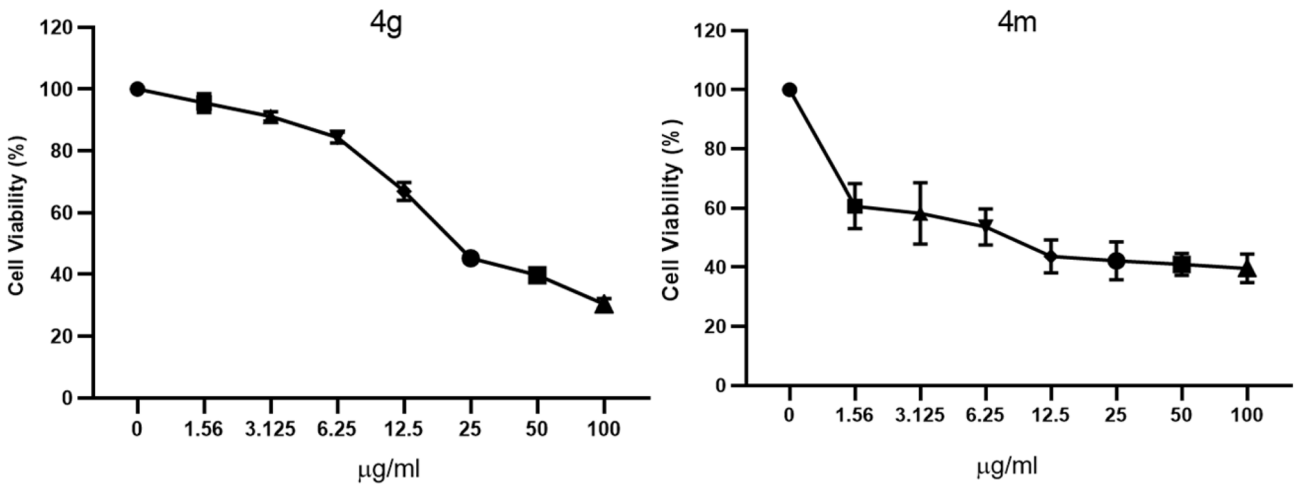

Fig. 7 Cytotoxic effects of compounds **4g**, and **4m** on the MCF-7 breast cancer cells.

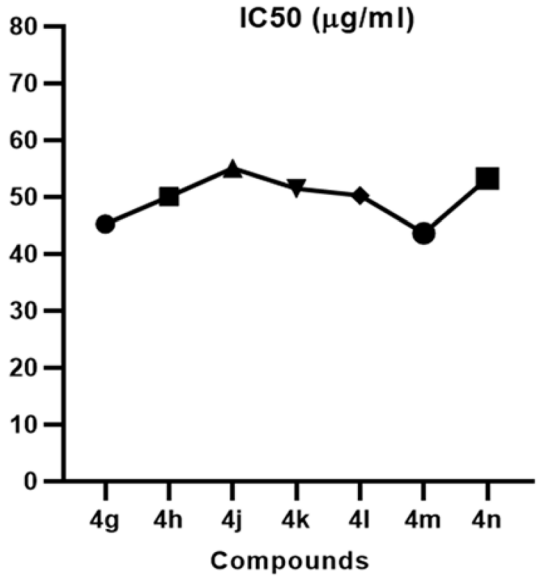

Fig. 8 IC_{50} values of (PHT) derivatives (**4g–4n**) against MCF-7 breast cancer cells.

and cell viability was assessed using the MTT assay. The IC_{50} values, defined as the concentration necessary to reduce cell viability by 50%, were calculated using GraphPad Prism 8 software. As summarized in (Table 4), the cytotoxic activities of the synthesized pyrene-hydrazinyl-thiazole (PHT) derivatives (**4g**, **4h**, **4j**, **4k**, **4l**, **4m**, and **4n**) against the MCF-7 human breast cancer cell line are presented. Cell viability was measured to ascertain the half-maximal inhibitory concentration (IC_{50}) after the substances were evaluated at graded concentrations (1.56–100 μg mL^{-1}). Doxorubicin was used as a reference standard in the MTT assay against MCF-7 cells to provide a benchmark for comparison of cytotoxic activity. Compound **4m** exhibited moderate anticancer activity compared to doxorubicin, indicating its potential as a promising lead scaffold.[61] Among the synthesized derivatives, compound **4m** with X = F, CF_3, had an IC_{50} of 43.66 μg mL^{-1}, closely followed by compound **4g** with X = OCH_3 (45.24 μg mL^{-1}), demonstrating their superior growth inhibitory effects (Fig. 7 and 8). While compounds **4j** (55.04 μg mL^{-1}) and **4n** (53.22 μg mL^{-1}) with X = diphenyl ring and F showed weaker activity, compounds **4h**, **4k**, and **4l** (X = CH_3SO_2, OCF_3, and CF_3) showed moderate activity with IC_{50} values of 50.04, 51.43, and 50.23 μg mL^{-1}, respectively.

The effect of structural differences within the PHT scaffold on anticancer activity is shown by the dose-dependent decrease in cell survival seen in all variants. The dose-dependent lethal effects of compounds **4g** and **4m** on MCF-7 breast cancer cells, as assessed by the MTT assay, are shown in (Fig. 7). Cell viability gradually decreased with increasing doses of both drugs (1.56–100 μg mL^{-1}), with **4m** showing a stronger inhibitory effect than **4g**, which is consistent with its lower IC_{50} value. These results confirm the strong growth-inhibitory potential of both derivatives, highlighting their ability to effectively suppress MCF-7 cell proliferation. In the (Fig. 8) presents the calculated IC_{50} values of the PHT derivatives (**4g–4n**) against MCF-7 cells. Among them, **4m** (43.66 μg mL^{-1}) and **4g** (45.24 μg mL^{-1}) displayed the strongest cytotoxic activity, whereas **4j** (55.04 μg mL^{-1}) and **4n** (53.22 μg mL^{-1}) exhibited comparatively weaker effects. The cytotoxic profiles of **4h**, **4j**, **4k**, **4l** and **4n** are provided in the SI (Fig. S4). Their weaker activities could be attributed to poor membrane permeability or unfavorable interactions with cellular targets, possibly arising from steric hindrance or less favorable electronic effects.

These findings suggest that structural variations among the synthesized molecules influence their cytotoxic potential, with compounds **4g** and **4m** emerging as promising leads for further development as anticancer agents against MCF-7 cells. In the SI (Fig. S6) illustrates the cytotoxic efficiency of synthesized derivatives **4g** and **4m** against the MCF-7 breast cancer cell line. In the control groups (untreated cells), a high density of viable cells with intact morphology is observed, indicating normal growth and proliferation. In contrast, the treated groups exposed to compounds **4g** and **4m** exhibit a marked reduction in viable cell count, accompanied by cell shrinkage, detachment, and morphological alterations characteristic of cytotoxic damage. These changes confirm the growth-inhibitory effects of both derivatives, consistent with the MTT assay data (Table 4), where **4g** (IC_{50} = 45.24 μg mL^{-1}) and **4m** (IC_{50} = 43.66 μg mL^{-1}) demonstrated significant cytotoxicity against MCF-7 cells. The microscopic evidence supports the conclusion that **4g** and **4m** effectively impair MCF-7 cell viability through dose-dependent cytotoxic mechanisms.

4 Conclusion

In conclusion, we have established an efficient, high-yield one-pot strategy for synthesis of some new library of pyrene-linked hydrazinyl-thiazole derivatives under mild and operationally convenient conditions, employing catalytic $InCl_3$ in an aqueous ethanol medium. This method offers several practical advantages, including short reaction times, excellent yields, broad functional group tolerance, and a chromatography-free isolation process that greatly enhances its scalability and synthetic utility. This protocol also enables the construction of complex heterocyclic frameworks in a single step, demonstrating the effectiveness of $InCl_3$ in promoting hydrazinyl-thiazole formation in mixed aqueous media. The biological screening results showed that compounds **4m** and **4g** with IC_{50} values of 43.66 and 45.24 μg mL^{-1} were the most effective against MCF-7 breast cancer cells, demonstrating significant cytotoxicity. Molecular docking studies further substantiated these observations by indicating strong binding affinities and stable interaction profiles within the target active site. These combined experimental and computational findings also elucidated key structure–activity relationship trends within the series. Overall, the results reinforce the potential of these derivatives as promising anticancer applications.

Author contributions

Pramod Dinkar Jawalepatil: conceptualized the research strategy and carried out the synthesis of compounds. Amol Maruti Jadhav: performed compound characterization, wrote the original manuscript draft, and prepared the SI. Pritam

Bhagwan Bhosale: conducted cytotoxicity studies. Pooja Singh: performed *in silico* studies and molecular docking. Hyun Ho Choi and Sang Yong Nam: supervised the project, guided data interpretation, and revised the manuscript. Satish U. Deshmukh: contributed to manuscript editing and scientific discussions. Mahesh N. Waman, and Gajanan N. Wadje: contributed to manuscript writing. All authors analyzed the results, reviewed, and approved the final version of the manuscript.

Conflicts of interest

There are no conflicts of interest to declare.

Data availability

Additional datasets generated and analyzed during the current study are available from the corresponding author on reasonable request.

All data supporting the findings of this study are available within the article and its supplementary information (SI). Supplementary information: experimental procedures, characterization data, and copies of NMR and LC-MS spectra for all synthesized compounds. See DOI: https://doi.org/10.1039/d5ra09880g.

Acknowledgements

This research was supported by Basic Science Research Program through the National Research Foundation of Korea (NRF) funded by the Ministry of Education (RS-2020-NR049575). This research was supported by the National Research Foundation of Korea (NRF) (2021M3H4A3A01043762).

References

1 R. A. Sheldon, *Green Chem.*, 2016, **18**, 3180–3183.
2 X. Shen, G. Hong and L. Wang, *Org. Biomol. Chem.*, 2025, **23**, 2059–2078.
3 G. Brahmachari, K. Nurjamal, I. Karmakar, S. Begam, N. Nayek and B. Manda, *ACS Sustainable Chem. Eng.*, 2017, **5**, 9494–9505.
4 C. G. Neochoritis, T. Z. Tzitzikas, K. K. Hodgetts and A. Domling, *J. Chem. Educ.*, 2020, **97**, 3739–3745.
5 D. G. Hall, T. Rybak and T. Verdelet, *Acc. Chem. Res.*, 2016, **49**, 2489–2500.
6 Y. Gu, *Green Chem.*, 2012, **14**, 2091–2128.
7 S. S. Acharya, B. K. Guin and B. B. Parida, *J. Org. Chem.*, 2025, **90**, 2717–2727.
8 K. B. Gangurde, R. A. More, V. A. Adole and D. S. Ghotekar, *J. Mol. Struct.*, 2024, **1299**, 136760.
9 Z. X. Niu, Y. T. Wang, S. N. Zhang, Y. Li, X. B. Chen, S. Q. Wang and H. M. Liu, *Eur. J. Med. Chem.*, 2023, **250**, 115172.
10 V. Kumari, S. S. Acharya, N. Mondal and L. H. Choudhury, *J. Org. Chem.*, 2024, **89**, 18003–18018.
11 R. Dahiya, S. Dahiya, N. K. Fuloria, S. Kumar, R. Mourya, S. V. Chennupati, S. Jankie, H. Gautam, S. Singh, S. K. Karan, S. Maharaj, S. Fuloria, J. Shrivastava, A. Agarwal, S. Singh, A. Kishor, G. Jadon and A. Sharma, *Mar. Drugs*, 2020, **18**, 329.
12 (*a*) M. Feng, B. Tang, S. H. Liang and X. Jiang, *Curr. Top. Med. Chem.*, 2016, **16**(11), 1200–1216; (*b*) S. Sharma, C. C. Malakar and V. Singh, *Asian J. Org. Chem.*, 2020, **9**, 1857–1868; (*c*) S. Sharma, D. Singh, S. Kumar, Vaishali, R. Jamra, N. Bansal, Deepika and C. C. Malakar, *Beilstein J. Org. Chem.*, 2023, **19**, 231–244.
13 M. S. Ebaid, H. A. A. Ibrahim, A. F. Kassem and A. Sabt, *RSC Adv.*, 2024, **14**, 36989–37018.
14 J. Sućˊ, I. Dokli and M. Gredičak, *Chem. Commun.*, 2016, **52**, 2071–2074.
15 T. Dzeha, M. J. Hall and J. G. Burgess, *Mar. Drugs*, 2022, **20**(2), 128.
16 A. Saeed, P. A. Channar, G. Shabir and F. A. Larik, *J. Fluoresc.*, 2016, **26**, 1067–1076.
17 P. Kosikowska and L. Berlicki, *Expert Opin. Ther. Pat.*, 2011, **21**, 945–957.
18 P. Kafarski and M. Talma, *J. Adv. Res.*, 2018, **13**, 101–113.
19 L. V. Modolo, A. X. de Souza, L. P. Horta, D. P. Araujo and A. de Fatima, *J. Adv. Res.*, 2015, **6**, 35–44.
20 H. Bektaş, S. Ceylan, N. Demirbaş, S. A. Karaoğlu and B. B. Sokmen, *Med. Chem. Res.*, 2013, **22**, 3629–3639.
21 M. Taha, N. H. Ismail, S. Imran, A. Wadood, F. Rahim, K. M. Khan and M. Riaz, *Bioorg. Chem.*, 2016, **66**, 80–87.
22 J. Das, P. Chen, D. Norris, R. Padmanabha, J. Lin, R. V. Moquin, Z. Shen, L. S. Cook, A. M. Doweyko, S. Pitt and S. Pang, *J. Med. Chem.*, 2006, **49**, 6819–6832.
23 A. Ayati, S. Emami, A. Shafiee and A. Foroumadi, *Eur. J. Med. Chem.*, 2015, **97**, 699–718.
24 V. A. Adole, T. B. Pawar and B. S. Jagdale, *J. Sulfur Chem.*, 2020, **42**, 131–148.
25 (*a*) Y. A. A. Mohammed, N. A. Kheder, M. S. Nafie, A. A. Abbas and K. M. Dawood, *RSC Adv.*, 2025, **15**, 30683–30696; (*b*) A. Paul, R. A. Khan, G. M. Shaik, D. S. Nesterov, M. F. C. Guedes da Silva and A. J. L. Pombeiro, *New J. Chem.*, 2024, **48**, 2907–2919; (*c*) A. Vignesh, A. Binoy, L. Thurakkal, N. S. P. Bhuvanesh, S. Sadhukhan and M. Porel, *J. Mol. Struct.*, 2024, **1295**, 136693.
26 (*a*) Y. Lin, H. Fan, Y. Li and X. Zhan, *Adv. Mater.*, 2012, **24**, 3087–3106; (*b*) H. J. Feng, P. H. Zhi and J. W. Wang, *Dyes Pigm.*, 2023, **220**, 111699.
27 H. Mehmood, T. Akhtar, M. Haroon, M. Khalid, S. Woodward, M. A. Asghar, R. Baby, R. Orfali and S. Perveen, *ACS Omega*, 2023, **8**, 11433–11446.
28 E. P. Gillis, K. J. Eastman, M. D. Hill, D. J. Donnelly and N. A. Meanwell, *J. Med. Chem.*, 2015, **58**, 8315–8359.
29 W. Zhu, J. Wang, S. Wang, Z. Gu, J. L. Aceña, K. Izawa, H. Liu and V. A. Soloshonok, *J. Fluorine Chem.*, 2014, **167**, 37–54.
30 C. Isanbor and D. O'hagan, *J. Fluorine Chem.*, 2006, **127**(3), 303–319.
31 E. Merino and C. Nevado, *Chem. Soc. Rev.*, 2014, **43**(18), 6598–6608.

32 E. L. Luzina and A. V. Popov, *Eur. J. Med. Chem.*, 2009, **44**, 4944–4953.
33 Y. Yang, S. Peng, S. Chen, F. Kang, J. Fan, H. Zhang, X. Yu, J. Li and Q. Zhang, *Nanoscale Horiz.*, 2024, **9**, 2198–2233.
34 M. Altarawneh and L. Ali, *Energy Fuels*, 2024, **38**(22), 21735–21792.
35 F. P. Kinik, A. O. Guerrero, D. Ongari, C. P. Ireland and B. Smit, *Chem. Soc. Rev.*, 2021, **50**, 3143–3177.
36 L. Piñeiro, M. Novo and W. Al-Soufi, *Adv. Colloid Interface Sci.*, 2015, **215**, 1–12.
37 Y. T. S. Steiner, G. M. Romano, L. Massai, M. Lippi, P. Paoli, P. Rossi, M. Savastano and A. Bencini, *Molecules*, 2023, **28**, 4552.
38 Q. X. Chen, K. Cheng, W. H. Wang, L. Yang, Y. S. Xie, L. Feng, J. Zhang, H. T. Zhang and H. Y. Sun, *J. Pharm. Anal.*, 2020, **10**, 490–497.
39 N. M. Khalifa, M. A. A. Omar, A. E. G. E. Amr and M. E. Haiba, *Int. J. Biol. Macromol.*, 2013, **54**, 51–56.
40 N. F. Zakirova, A. V. Shipitsyn, M. V. Jasko, M. M. Prokofjeva, V. L. Andronova, G. A. Galegov, V. S. Prassolov and S. N. Kochetkov, *Bioorg. Med. Chem.*, 2012, **20**, 5802–5809.
41 F. Biemar and M. Foti, *Cancer Biol. Med.*, 2013, **10**(4), 183–186.
42 R. Naser, H. Dilabazian, H. Bahr, A. Barakat and M. El-Sibai, *Oncol. Rep.*, 2022, **48**, 190.
43 I. Soerjomataram and F. Bray, *Nat. Rev. Clin. Oncol.*, 2021, **18**, 663–672.
44 P. Devakrishnan, N. M. Nasir, J. Stanslas, M. A. M. Latif, A. Z. Ismail and F. F. Baharuddin, *Results Chem.*, 2025, **13**, 101998.
45 K. Jalal, K. Khan, D. J. Haleem and R. Uddin, *J. Mol. Struct.*, 2022, **1254**, 132244.
46 I. M. Hâncu, S. Giuchici, A. V. F. Linţa, B. Lolescu, A. Sturza, D. M. Muntean, M. D. Dănilă and R. Lighezan, *Mol. Cell. Biochem.*, 2025, **480**, 3225–3252.
47 S. Gaur, M. E. Gross, C. P. Liao, B. Qian and J. C. Shih, *Prostate*, 2019, 1–11.
48 S. W. Hong, A. Heydari, P. R. Watson, P. H. Teesdale-Spittle, R. Page, P. T. Northcote, R. A. Keyzers, M. Vyssotski and P. Truman, *Chem.-Biol. Interact.*, 2025, **413**, 111477.
49 W. Hernández, F. Carrasco, A. Vaisberg, E. Spodine, M. Icker, H. Krautscheid and P. O. Gonzales, *J. Chem.*, 2023, 5413236.
50 N. A. Khaled, N. S. Ahmed, A. Z. Abdelazem, N. A. Mohamed, A. F. El-Sayed and S. A. Ahmed, *J. Mol. Struct.*, 2023, **1288**, 135753.
51 A. H. Jawhari, Y. E. Mukhrish, A. F. El-Sayed and R. E. Khidre, *Curr. Org. Chem.*, 2023, **27**, 860–875.
52 K. Raval and T. Ganatra, *Pharmacology*, 2022, **7**, 12–16.
53 (*a*) P. A. Channar, A. Saeed, S. Afzal, D. Hussain, M. Kalesse, S. A. Shehzadi and J. Iqbal, *Mol. Diversity*, 2021, **25**, 787–799; (*b*) U. Salar, K. M. Khan, S. Syed, M. Taha, F. Ali, N. H. Ismail, S. Perveen, A. Wadood and M. Ghufran, *Bioorg. Chem.*, 2017, **70**, 199–209.
54 (*a*) A. Das, S. Dey, S. Chakraborty, A. Barman, R. N. Yadav, R. Gazi, M. Jana and M. F. Hossain, *ChemistrySelect*, 2021, **6**, 9552–9558; (*b*) M. Tudose, R. D. Baratoiu-Carpen, E. M. Anghel, M. Voicescu, S. Somacescu, D. C. Culita, A. Hanganu, A. Kuncser and A. Radoi, *Mater. Chem. Phys.*, 2021, **262**, 124315; (*c*) T. S. Choudhare, D. S. Wagare, V. T. Kadam, A. A. Kharpe and P. D. Netankar, *Polycyclic Aromat. Compd.*, 2023, **43**, 2672–2679; (*d*) S. Dey, A. Das, R. N. Yadav, P. J. Boruah, P. Bakli, T. Baishya, K. Sarkar, A. Barman, R. Sahu, B. Maji, A. K. Paul and M. F. Hossain, *Org. Biomol. Chem.*, 2023, **21**, 1771–1779; (*e*) A. Aggarwal and H. K. Chopra, *Res. Chem. Intermed.*, 2025, **51**, 3301–3316.
55 (*a*) A. M. Jadhav, S. G. Balwe, J. S. Kim, K. T. Lim and Y. T. Jeong, *Tetrahedron Lett.*, 2019, **60**, 560–565; (*b*) R. Shah, R. Kamani, D. Raval, K. Patel, V. Prajapati, R. Prajapati, S. Dongre, U. Shah and A. Patel, *Sci. Rep.*, 2025, **15**, 31412; (*c*) B. Coetzee, S. J. Cloete, A. Petzer, J. P. Petzer and T. T. Cloete, *Med. Chem. Res.*, 2025, **34**, 1903–1913.
56 D. M. Eliman, A. A. Elgazar, F. F. Senduny, R. A. El-Domany, F. A. Badria and W. M. Eldehna, *J. Enzyme Inhib. Med. Chem.*, 2022, **37**, 39–22.
57 J. C. Stockert, R. W. Horobin, L. L. Colombo and A. Blázquez-Castro, *Int. J. Mol. Sci.*, 2021, **22**, 794.
58 (*a*) M. Gajewska, A. Sobolewska, R. Kozłowski and T. Motyl, *Cancers*, 2020, **12**, 3509; (*b*) X. Dai, H. Cheng, Z. Bai and J. Li, *Breast Cancer Res.*, 2017, **19**, 71; (*c*) Ş. Comşa, A. M. Cîmpean and M. Raica, *J. Cell. Mol. Med.*, 2020, **24**, 4060–4076; (*d*) S. Zarougui, A. El-Rajy, A. Faris, H. Imtara, M. El Fadili, A. A. Qurtam, F. A. Nasr, M. Al-Zharani and M. Elhallaoui, *Front. Chem.*, 2024, **12**, 1384832; (*e*) Q. Xu, X. Li and Y. Jia, *Front. Pharmacol*, 2025, **16**, 1467504.
59 (*a*) R. Marcotte, A. Sayad, K. R. Brown, *et al.*, *Nat. Commun.*, 2022, **13**, 725; (*b*) S. Zarougui, M. Er-Rajy, A. Faris, H. Imtara, M. El Fadili, A. A. Qurtam, F. A. Nasr, M. Al-Zharani and M. Elhallaoui, *Front. Chem.*, 2024, **12**, 1384832.
60 D. L. Holliday and V. Speirs, *Breast Cancer Res.*, 2011, **13**, 215.
61 (*a*) S. Ramazi, M. Salimian, A. Allahverdi, S. Kianamiri and P. Abdolmaleki, *Sci. Rep.*, 2023, **13**, 8844; (*b*) H. I. Abdelaal, A. R. Mohamed, M. F. Abo-Ashour, S. Giovannuzzi, S. H. Fahim and H. A. Abdel-Aziz, *Bioorg. Chem.*, 2024, **152**, 107759; (*c*) H. Effat, H. A. Abosharaf and A. M. Radwan, *Sci. Rep.*, 2024, **14**, 2824.